

# Probabilistic Estimation of Chirp Instantaneous Frequency Using Gaussian Processes

Zheng Zhao, *Student Member, IEEE*, Simo Särkkä, *Senior Member, IEEE*, Jens Sjölund,  
and Thomas B. Schön, *Senior Member, IEEE*

**Abstract**—We present a probabilistic approach for estimating chirp signal and its instantaneous frequency function when the true forms of the chirp and instantaneous frequency are unknown. To do so, we represent them by joint cascading Gaussian processes governed by a non-linear stochastic differential equation, and estimate their posterior distribution by using stochastic filters and smoothers. The model parameters are determined via maximum likelihood estimation. Theoretical results show that the estimation method has a bounded mean squared error. Experiments show that the method outperforms a number of baseline methods on a synthetic model, and we also apply the method to analyse a gravitational wave data.

**Index Terms**—chirp signal, frequency estimation, frequency tracking, instantaneous frequency, state-space methods, Gaussian process, Kalman filtering, smoothing, automatic differentiation

## I. INTRODUCTION

Chirp signals are elementary and ubiquitous objects in signal processing. We consider a real-valued chirp signal  $y: [0, \infty) \rightarrow \mathbb{R}$  of the form

$$y(t) = \alpha(t) \sin\left(\phi_0 + 2\pi \int_0^t f(s) ds\right), \quad (1)$$

where  $\alpha: [0, \infty) \rightarrow \mathbb{R}$ ,  $\phi_0 \in \mathbb{R}$ , and  $f: [0, \infty) \rightarrow [0, \infty)$  stand for the instantaneous amplitude, initial phase, and instantaneous frequency (IF) function of  $y$ , respectively. The integral of  $f$  in the equation above is referred to as the phase function [1, 2]. Estimating IF from measurements of a chirp signal is important in a number of real-world applications, such as radar tracking [3], communications [4], frequency modulation [5], seismic attributes [6, 7], and astronomy [8].

The goal of this paper is to estimate the IF function  $f$  in terms of posterior distribution from evenly or unevenly sampled noisy measurements of  $y$  contaminated by independent Gaussian noises. Importantly, we do *not* assume that the form of the IF function  $f$  or amplitude  $\alpha$  is explicitly known. This relaxation of the assumptions is desirable, as in reality

it is hard to obtain the exact forms of these functions except for a few isolated cases. For instance, to estimate Doppler frequency in radar tracking, one must know the dynamics of the tracking object to formulate  $f$ . The amplitude  $\alpha$  may also be contaminated by some unknown random noises or damping factors as well [9–11]. In this introduction, we start by a short literature review on existing IF estimation methods, then, we elucidate the essence of our approach and explain its novelty and our contributions.

The simplest IF estimation method is arguably to use the Hilbert transform [1]. The principle of this method is to find the instantaneous phase of the analytic representation of the signal at hand – which is the Hilbert transform of the signal – and then to compute the IF by differentiating the (unwrapped) instantaneous phase. However, the applicability of this method is limited in the sense that it only works well for clean signals. Another commonly used method is based on time-windowed power spectrum [1, Eq. 22]. The idea is to estimate the power spectral densities of the signal over time-window segments, then at each window-segment time, the IF is approximated from the first moment by taking the power spectral density at that time as distribution. However, these spectrogram-based methods require human experts to manually tune parameters (e.g., window type, length, and overlap), and the estimation in time-frequency domain is restricted by Gabor’s uncertainty principle [12]. This method also needs interpolation to deal with unevenly sampled measurements.

A notable class of IF estimation methods is based on parametrisation of IF. Namely, one postulates a parametrised form of IF and then estimates its parameters using, for example, maximum likelihood estimation [13, 14]. In literature, the affine parametrisation is commonly used [14–19], yielding quadratic-phase chirps. This affine assumption is indeed useful in many applications, such as radars. Furthermore, thanks to its affine structure and limited number of parameters, it is possible to develop computationally efficient (but on the other hand ad-hoc) methods to estimate these parameters [see, e.g., 14, 18]. Using polynomials to model IF is widely used as well [14, 20–24]. However, one downside of the parametric approach is that the parametrisation can be over/mis-specified and it is hard to generalise. As an example, in radar tracking, the affine assumption is true only if the tracking object is moving in constant radial acceleration. It is challenging to find a precise parametrisation when the manoeuvring dynamics of the tracking object is unknown [21]. As for the polynomial approach, it is difficult to determine the degree of polynomials, and the estimation of the polynomial coefficients may

Zheng Zhao, Jens Sjölund, and Thomas B. Schön were with Department of Information Technology, Uppsala University, Sweden (e-mail: zheng.zhao@it.uu.se).

Simo Särkkä was with Department of Electrical Engineering and Automation, Aalto University, Finland.

This research was partially supported by the Wallenberg AI, Autonomous Systems and Software Program (WASP) funded by Knut and Alice Wallenberg Foundation and by Kjell och Märta Beijer Foundation.

The computations handling was enabled by resources provided by the Swedish National Infrastructure for Computing (SNIC) at NSC partially funded by the Swedish Research Council through grant agreement no. 2018-05973.

Manuscript received \*\* \*\*, \*\*\*\*; revised \*\* \*\*, \*\*\*\*.

encounter side effects as well, such as numerical instability, optima oscillation, aliasing, and phase unwrapping [21, 23].

Apart from the parametric approaches, one can also put a prior (e.g., Gaussian process) on the IF and then make use of Bayesian estimators to find the posterior distribution of the IF. This relaxes the ambiguities caused by the aforementioned parametric approaches to a certain extent. Moreover, since signals are temporal functions, it makes sense to consider Markov priors (e.g., state-space models) in favour of efficient computations. Early work using this idea dates back to [25, pp. 99], where the phase or IF was modelled by linear stochastic differential equations. Essentially, this class of approaches and its variants (in the discrete-time representation) use a state-space model of the form

$$\begin{aligned} f(t_k) &= A_{k-1} f(t_{k-1}) + Q(t_{k-1}), \\ Y_k &= \alpha \sin\left(\phi_0 + 2\pi \int_0^{t_k} f(z) dz\right) + \xi_k, \end{aligned} \quad (2)$$

for time steps  $k = 1, 2, \dots$ , where  $\{A_k\}_{k \geq 0}$  and  $\{Q_k\}_{k \geq 0}$  are scalar coefficients and Gaussian random variables, respectively,  $\{\xi_k\}_{k=1}$  are independent Gaussian noises, and  $\{Y_k\}_{k=1}$  stand for the measurements of the chirp signal.

Furthermore, one can cancel out the sine function and  $f$ 's integral in Equation (2) by using a harmonic equation representation, yielding an approximate augmented non-linear dynamic model and linear measurement model [see, 26, pp. 2]. Then, one can apply non-linear filters, such as extended Kalman filters (EKFs) [26–30], sigma-point filters [31], particle filters [32, 33], and Gaussian-sum filters [34] to approximate the posterior distribution of  $f$ . However, these methods can result in model ambiguities as well, since real-world chirp signals are not always well-described by the simple measurement model in Equation (2). For example, elastic signals have damped amplitude; amplitude can be distorted by a random nuisance process [9–11]. To tackle this problem, we can put a prior on the chirp signal as well, then estimate the joint posterior distribution of both the IF and chirp. This is one of the essence in this paper, and we shall see that our model is essentially a continuous and stochastic extension of Equation (2) in a different flavour and view of the problem.

There are also other classical IF estimators, for instance, the adaptive notch filters (ANFs) [35, 36]. These ANF-based methods are sensitive to signal-noise-ratio. As in [35, 36], the variance of the IF estimate increases linearly in the variance of measurement noise.

### A. Contributions

In this paper, we view chirp signals and IFs as realisations drawn from a stochastic process composed of multiple Gaussian processes (GPs) which are ubiquitous models in the statistics and machine learning communities [37]. Specifically, we design a family of (non-stationary) harmonic GPs that are suitable for modelling a wide range of chirp signals. These GPs are governed by a stochastic differential equation (SDE), and their IF parameters are driven by SDE-GPs as well. In a modern interpretation, this design results in a hierarchical statistical model that is a special case of the deep Gaussian

processes [38, 39, pp. 82]. This model is particularly useful when the true forms of the chirp and its IF are unknown. Since the model is formulated in SDEs, this allows us to approximate the posterior distribution of chirp and IF in both continuous and discrete times, by applying non-linear stochastic filters and smoothers, such as sigma-point/particle filters. Moreover, the model parameters – which control the characteristics of the latent chirp and IF – can be automatically determined using maximum likelihood estimation<sup>1</sup>.

Based on this model, we theoretically show that for a class of chirp signals, IF functions, and Gaussian filters, the IF estimates are bounded in the mean square sense. We also from synthetic experiments demonstrate that IF estimation using this model outperform a number of baseline methods. Lastly, we apply our model to estimate the IF of a gravitational wave signal from real data.

### B. Structure

This paper is organised as follows. In Section II, we show how to view the IF estimation problem as a GP regression problem. In the same section, we show how to choose a pair of GP priors appropriately so as to jointly model chirp signals and IFs, and solve the estimation problem by using state-space methods. Theoretical result and numerical experiment are presented in Sections III and IV, respectively, followed by the conclusions in Section V.

## II. CHIRP AND INSTANTANEOUS FREQUENCY AS GAUSSIAN PROCESSES

We consider the following GPs for modelling chirp signals and their IFs whose exact forms are unknown. Let us define a (non-stationary) GP  $X: [0, \infty) \rightarrow \mathbb{R}^{d_x}$  by

$$X(t) \sim \text{GP}(m_X(t; f), C_X(t, t'; f)) \quad (3)$$

for some suitably selected mean  $m_X(t; f) = \mathbb{E}[X(t) | f]$  and covariance functions  $C_X(t, t'; f) = \text{Cov}[(X(t) - m_X(t))(X(t') - m_X(t'))^T | f]$  parametrised by its IF  $f$ . One can then use this GP  $X$  to represent chirp signals by any linear transformation  $\mathbb{R}^{d_x} \rightarrow \mathbb{R}$ . As for the IF  $f$ , we consider it driven by a GP as well, in the way that

$$\begin{aligned} f(t) &:= g(V(t)), \\ V(t) &\sim \text{GP}(0, C_V(t, t')), \end{aligned} \quad (4)$$

where  $V$  is a zero-mean GP that completely characterises  $f$  under a positive bijection  $g: \mathbb{R} \rightarrow \mathbb{R}_{>0}$ . The reason for introducing  $g$  is to ensure that the IF is positive, for instance, by using  $g(\cdot) = \exp(\cdot)$ , or  $g(\cdot) = \log(1 + \exp(\cdot))$ . Due to this,  $f$  is technically not a GP but its driving term  $V$  is. Unless otherwise stated, we might refer  $f$  as a GP for simplicity. One can also use  $g$  for other purposes as well, for example, to introduce the carrier frequency in frequency modulation by adding a constant offset in  $g$ .

We let the random variable  $Y_k \in \mathbb{R}$  represent the noisy measurement of  $X$  at any time  $t_k$ :

$$Y_k = H_X X(t_k) + \xi_k,$$

<sup>1</sup>Our implementation is published at <https://github.com/spdes/chirpgp>.

where  $H_X: \mathbb{R}^{d_x} \rightarrow \mathbb{R}$  is the linear operator that extracts the chirp from  $X$ , and  $\xi_k \sim \mathcal{N}(0, \Xi)$ . Suppose that we have a set of measurements  $y_{1:T} := \{y_k\}_{k=1}^T$  at hand, the goal is then to estimate the joint posterior density

$$p_{X(t), V(t)}(x, v \mid y_{1:T}) \quad (5)$$

of  $X(t)$  and  $V(t)$  marginally for all  $t \in [0, \infty)$ .

In practice, solving the estimation problem in Equation (5) is difficult. The main difficulty lies in how to find a concrete pair of mean  $m_X$  and covariance  $C_X$  functions such that  $X$  is a reasonable prior for chirp signals. By “reasonable”, we mean that the samples from  $X$  should be valid chirp signals of the form in Equation (1). The other difficulties consist in the intractability and expensive computation of Equation (5), as the joint prior model of  $X$  and  $f$  is not a GP but a hierarchical/deep GP [see, e.g., 38].

In what follows, we give solutions to tackle these difficulties. Specifically, in Section II-A we construct  $X$  via a class of harmonic non-stationary SDE-GPs; in Section II-B, we leverage this type of SDE-GPs to formulate a continuous-discrete state-space model that we use to estimate the posterior distribution (5) by applying non-linear filters and smoothers. In Section II-C, we exemplify Gaussian filters and smoothers, and their log-likelihood for estimating the model parameters.

#### A. Chirp signal prior

In light of the periodic nature of chirp signals, it seems natural to think of using the periodic covariance function (see its formulation in [37, pp. 92] or [40]) for  $C_X$  to construct the prior GP  $X$  in Equation (3). However, this periodic covariance function is not amenable to use instantaneous frequency, as the function fails to be positive definite when its frequency parameter is time-dependent. Moreover, even if we have found a valid and meaningful  $C_X$ , the computation for obtaining the posterior distribution (5) is demanding because the matrix inversion of the covariance matrix has cubic complexity in the number of measurements. Indeed there are sparse pseudo-input methods to approximate full-rank GP covariance matrix [41, 42], however, one must be cautious in using them for the IF estimation, since these sparse approximations introduce down-samplings. Moreover, the down-sampling rates are not easy to control, as their pseudo-inputs (i.e., down-sampling points) are placed by an optimisation procedure [41]. In order to approximate the posterior density (5), one often also needs, for instance, variational Bayes [43] or Markov Chain Monte Carlo [44, 45] methods which can be computationally expensive as well. These matters make it difficult to deal with lengthy signals, such as audio recordings.

Therefore, we choose to construct  $X$  via linear stochastic differential equations (SDEs), the solutions of which are (Markov) GPs with *implicitly* defined  $C_X$  [46, 47]. This relieves us from *explicitly* designing a valid covariance function  $C_X$  and solving the covariance matrix inversion. Choosing this Markov type of priors makes sense, because the desired posterior density (5) is marginal in time (i.e., we can solve it sequentially in time without using the full covariance matrix).

To see how this SDE is formulated, let us first consider a simple class of harmonic GPs [48] that carries sinusoidal

signals with a *constant* frequency  $f$ . These harmonic GPs are governed by linear time-invariant SDEs of the form

$$\begin{aligned} dX(t) &= \begin{bmatrix} -\lambda & -2\pi f \\ 2\pi f & -\lambda \end{bmatrix} X(t) dt + b dW_X(t), \\ X(0) &\sim \mathcal{N}(m_0^X, P_0^X), \end{aligned} \quad (6)$$

where  $X: [0, \infty) \rightarrow \mathbb{R}^2$  stands for the state,  $W_X: [0, \infty) \rightarrow \mathbb{R}^2$  is a standard Wiener process (with unit spectral density), and  $b \in \mathbb{R}$  is the dispersion coefficient. The parameter  $\lambda$  is a positive damping constant representing the loss of energy which is present in a number of real signals, such as seismic waves and elastic dynamics. This SDE has an analytical solution [46], specifically, starting at any initial time  $s \in [0, \infty)$ , the solution at any  $t \geq s$  is

$$X(t) = F(t, s) X(s) + Q(t, s), \quad (7)$$

where

$$\begin{aligned} F(t, s) &= \exp\left((t-s) \begin{bmatrix} -\lambda & -2\pi f \\ 2\pi f & -\lambda \end{bmatrix}\right) \\ &= \begin{bmatrix} \cos((t-s)2\pi f) & -\sin((t-s)2\pi f) \\ \sin((t-s)2\pi f) & \cos((t-s)2\pi f) \end{bmatrix} e^{-\lambda(t-s)}, \\ Q(t, s) &= b \int_s^t F(t, z) dW_X(z). \end{aligned}$$

The marginal distribution of  $Q$  is Gaussian, that is,  $Q(t, s) \sim \mathcal{N}(0, \Sigma(t, s))$ , and its covariance reads

$$\begin{aligned} \Sigma(t, s) &:= \text{Cov}[Q(t, s)] \\ &= b^2 \int_s^t F(t, z) F(t, z)^\top dz \\ &= \begin{cases} b^2 (1 - \exp(-2\lambda(t-s))) / (2\lambda) I_2, & \lambda \neq 0, \\ b^2 (t-s) I_2, & \lambda = 0, \end{cases} \end{aligned}$$

where  $I_2 \in \mathbb{R}^{2 \times 2}$  stands for the identity matrix. In what follows, we also interchangeably use the notation  $\Sigma(\Delta)$ , since  $\Sigma$  only depends on the time difference  $\Delta = t - s$ .

The solution process  $X$  in Equation (7) is a suitable prior for modelling sinusoidal signals in the sense that its statistics (i.e., mean and covariance) have periodic structures. It is well-known [46] that the mean and covariance functions of  $X$ , as per the form in Equation (3), are

$$m_X(t) = \mathbb{E}[X(t)] = F(t, 0) m_0^X$$

and

$$\begin{aligned} C_X(t, t') &= \text{Cov}[X(t), X(t')] \\ &= \begin{cases} \text{Cov}[X(t)] F(t', t)^\top, & t < t', \\ F(t, t') \text{Cov}[X(t')], & t \geq t', \end{cases} \end{aligned} \quad (8)$$

$$\text{Cov}[X(t)] = F(t, 0) P_0^X F(t, 0)^\top + \Sigma(t, 0),$$

respectively. From these, we can see that the mean

$$\mathbb{E} \begin{bmatrix} 0 & 1 \end{bmatrix} X(t) = \alpha e^{-\lambda t} \sin(\phi_0 + 2\pi f t)$$

is a damped sinusoidal signal with the frequency parameter  $f$ , amplitude  $\alpha = \|X(0)\|_2$ , and initial phase  $\phi_0 = \arctan(X_1(0) / X_2(0))$ . As for the covariance function  $C_X$ , we plot an example in Figure 1 at a frequency  $f = 0.5$  Hz. This figure clearly shows that this  $C_X$  has a periodic structure determined by  $f$ .

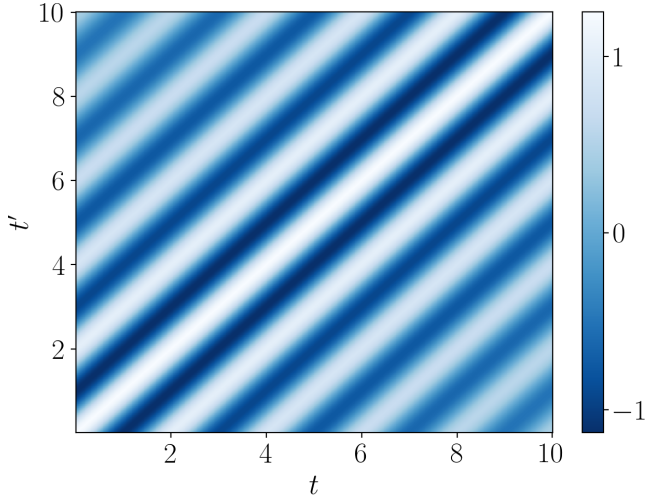


Figure 1. Covariance function  $C_X$  in Equation (8) evaluated at Cartesian  $[0, 10] \times [0, 10]$ . The parameters used are  $f = 0.5$  Hz,  $\lambda = 0.1$ ,  $b = 0.5$ , and  $P_0^X = 1.25 I_2$ . It is clear to see the periodic structure, and the fading effect on the anti-diagonal (from top-left to bottom-right) due to the damping factor.

### B. Model formulation

The SDE construction of  $X$  in Equation (6) allows for using time-dependent instantaneous frequency by directly substituting its constant frequency parameter  $f$  with a time-varying one, for instance, a GP as per Equation (4). This is valid because if doing so, the conditional mean of  $X$  becomes  $\mathbb{E}[X(t) | f(t)] = \alpha e^{-\lambda t} \begin{bmatrix} \cos(\phi_0 + 2\pi \int_0^t f(s) ds) & \sin(\phi_0 + 2\pi \int_0^t f(s) ds) \end{bmatrix}$  which matches the desired form as in Equation (1). As for the conditional covariance, it is not available in closed-form. We numerically plot an example of the conditional covariance in Figure 2.

In order to be consistent with the SDE construction of  $X$ , we need to represent  $V$  via an SDE as well. This means that we construct  $V$  from an SDE representation  $\bar{V}: [0, \infty) \rightarrow \mathbb{R}^{d_v}$  governed by

$$\begin{aligned} d\bar{V}(t) &= M \bar{V}(t) dt + L dW_V(t), \\ \bar{V}(0) &\sim N(0, P_0^V), \end{aligned} \quad (9)$$

where  $W_V: [0, \infty) \rightarrow \mathbb{R}$  is another standard Wiener process independent of  $W_X$ . We extract  $V$  from the state  $\bar{V}$  by  $V(t) = \bar{H}_V \bar{V}(t)$  for some linear operator  $\bar{H}_V: \mathbb{R}^{d_v} \rightarrow \mathbb{R}$ . The SDE coefficients  $M \in \mathbb{R}^{d_v \times d_v}$  and  $L \in \mathbb{R}^{d_v}$  need to be chosen appropriately so as to model the true IF at hand. One common choice is to let  $V$  be a Matérn GP. The Matérn GPs are useful in the sense that they are generic priors for modelling continuous functions with varying degree of regularity, and that their SDE representations are available in closed-form [47]. As an example, suppose that the latent IF is continuously differentiable, then we can let

$$\begin{aligned} M &= \begin{bmatrix} 0 & 1 \\ -3/\ell^2 & -2\sqrt{3}/\ell \end{bmatrix}, \quad L = \begin{bmatrix} 0 \\ 2\sigma(\sqrt{3}/\ell)^{3/2} \end{bmatrix}, \\ P_0^V &= \begin{bmatrix} \sigma^2 & 0 \\ 0 & 3\sigma^2/\ell^2 \end{bmatrix}, \quad \bar{H}_V = \begin{bmatrix} 1 & 0 \end{bmatrix}, \end{aligned} \quad (10)$$

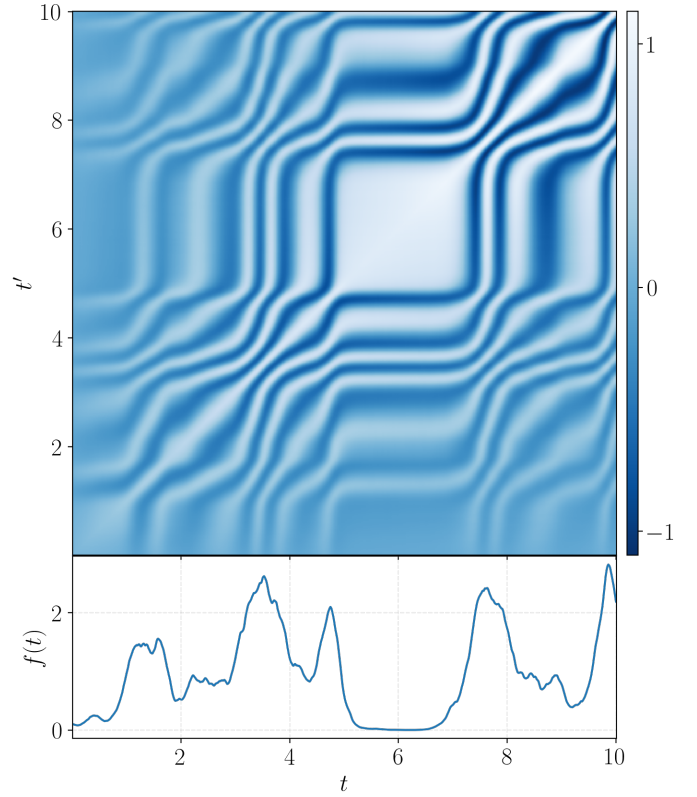


Figure 2. Top: covariance function of  $HU$  in SDE (11) by conditioning on a realisation of  $f$ . Bottom: the realisation of  $f$ . From the plot we can see that the periodicity changes over time driven by the value of  $f$ . Note that this covariance function is not analytically tractable, hence, we approximate it by Monte Carlo simulations.

and  $\bar{V}(t) = [V(t) \quad dV(t)/dt]^T \in \mathbb{R}^2$ , so that  $V$  is a Matérn ( $\nu = 3/2$ ) GP under the covariance function

$$\begin{aligned} C_V(t, t') &= \frac{\sigma^2 2^{1-\nu}}{\Gamma(\nu)} \psi(t, t')^\nu K_\nu(\psi(t, t')), \\ \psi(t, t') &:= \frac{\sqrt{2\nu} |t - t'|}{\ell}, \end{aligned}$$

where  $\ell$  and  $\sigma$  are the length and magnitude scale parameters (i.e., they determine the horizontal and vertical degrees of change of  $V$ ),  $\nu$  defines the smoothness of  $V$ , and  $K_\nu$  is the modified Bessel function of the second kind.

For simplicity of exposition, we will keep using the Matérn  $3/2$  setting as in Equation (10) in what follows. However, it is straightforward to use other classes of GPs as well by changing the SDE coefficients in Equation (9). We refer the readers to, for example, [39, 47] for how to do so.

Now let us substitute the parameter  $f$  in Equation (6) by  $f = g(V(t))$ , and define  $U(t) := [X(t) \quad \bar{V}(t)]^T \in \mathbb{R}^4$  as the joint state of  $X(t)$  and  $\bar{V}(t)$ . By concatenating the SDEs of  $X$  and  $\bar{V}$ , we eventually arrive at the following non-linear state-space chirp IF estimation model.

$$\begin{aligned} dU(t) &= A(U(t)) dt + B dW(t), \\ U(0) &\sim p_{U(0)}(u), \\ Y_k &= H U(t_k) + \xi_k, \end{aligned} \quad (11)$$

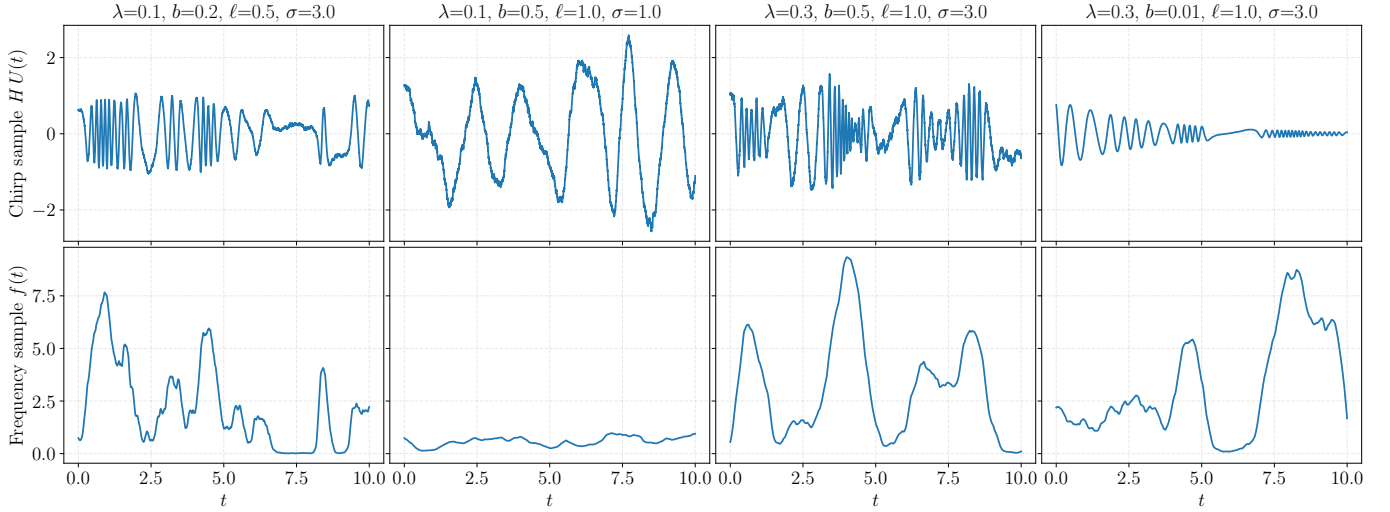


Figure 3. Samples drawn from the chirp-IF prior SDE (11) under four combinations of model parameters. We can see that the chirp frequency changes instantaneously based on the value of  $f$ , and that the model can be used to generate a rich variety of randomised chirp signals by tuning the model parameters. In this example, we let  $f(t) = \log(1 + \exp(V(t)))$ .

where the drift and dispersion functions are defined by

$$A(U(t)) := \begin{bmatrix} -\lambda & -2\pi g(V(t)) & 0 & 0 \\ 2\pi g(V(t)) & -\lambda & 0 & 0 \\ 0 & 0 & 0 & 1 \\ 0 & 0 & -3/\ell^2 & -2\sqrt{3}/\ell \end{bmatrix} U(t)$$

and

$$B := \begin{bmatrix} b & 0 & 0 \\ 0 & b & 0 \\ 0 & 0 & 0 \\ 0 & 0 & 2\sigma(\sqrt{3}/\ell)^{3/2} \end{bmatrix},$$

respectively, and the Wiener process  $W(t) := [W_X(t) \ W_V(t)]^T \in \mathbb{R}^3$ . The measurement operator  $H := [0 \ 1 \ 0 \ 0]$  aims to extract the second component of  $X$  from  $U$  so as to produce chirp signals of the form in Equation (1). The initial distribution can be assigned as a Gaussian  $p_{U(0)}(u) = \mathcal{N}(u | m_0, P_0)$ , where  $m_0$  and  $P_0$  are given by the initial means and covariances of  $X$ 's and  $V$ 's.

To see that the SDE in Equation (11) is an appropriate prior for modelling chirp signals with time-dependent IF, we can investigate the statistics of this SDE. In the beginning of this section, we have already mentioned that the conditional mean  $\mathbb{E}[HU(t) | f(t)]$  is a valid chirp signal of the form in Equation (1). Now we show the covariance function of  $HU$  by conditioning on a realisation of  $f$  in Figure 2. Compared to the covariance function  $C_X$  with a fixed frequency plotted in Figure 1, one can see that the (white) stripes in Figure 2 wiggle in time based on the value of  $f$ . This represents the change of instantaneous periodicity driven by the process  $f$ .

Another way to see the statistics of the SDE in Equation (11) is by looking at its samples. It is worth noting that the commonly-used Euler–Maruyama scheme is unstable in this case due to the SDE's non-linearity and the stiffness of Equation (6). There are a number of alternative simulators, such as Itô–Taylor expansions [49, 50], and locally conditional

discretisation (LCD) [39, pp. 77] thanks to this SDE's hierarchical structure. In Figure 3, we exemplify a few samples drawn from SDE (11) by using the LCD method under four combinations of model parameters (i.e.,  $\lambda, b, \ell$ , and  $\sigma$ ). From this figure, it is clear that we can generate a variety of chirp signals and IFs by tuning the model parameters, therefore, it is natural to estimate these parameters from chirp measurements data so as to mimic the characteristics of the true latent chirp signal. The parameters  $\lambda$  and  $b$  govern the damping factor and stochastic volatility of the chirp, while  $\ell$  and  $\sigma$  control the characteristics of the IF.

### C. Estimate the posterior distribution and model parameters

Following the state-space model in Equation (11), it is clear that solving the posterior density

$$p_{U(t)}(u | y_{1:T}), \quad \text{for all } t \in [0, \infty), \quad (12)$$

is essentially a (continuous-discrete) stochastic filtering and smoothing problem [47, 51]. Although this posterior distribution is intractable, there exist a plethora of approximate schemes, such as Gaussian filters and smoothers [52, 53], and particle filters and smoothers [54]. The distribution can be solved in both continuous-time and discrete-time. Furthermore, estimating the model parameters can be accomplished by optimising the marginal log-likelihood from the filtering posterior estimates.

At this stage, it is worth mentioning that this framework for estimating chirp IF is similar to that of [25–27], except that we formulate the problem from the GP point of view, and that our model is stochastic and continuous. More specifically, the model in [25–27] is a special case of SDE (11) when choosing  $b = 0$  and discretised using the LCD discretisation.

For the sake of pedagogy and the error analysis in Section III, we show a concrete solution to the posterior distribution (12) using the generic Gaussian filters and smoothers (GFSs) [52, 55]. We choose GFSs for the demonstration

because they generalise extended and sigma-points Kalman filters and smoothers which are commonly used in the signal processing community. These are shown in the following algorithm.

**Algorithm 1** (Gaussian filtering and smoothing for the chirp and IF estimation model in Equation (11)). *Find a Gaussian approximation to the SDE solution in Equation (11) in discrete-time such that*

$$U_k \approx \Phi(U_{k-1}) + \omega(U_{k-1}), \quad \omega(U_{k-1}) \sim \mathcal{N}(0, \Omega(U_{k-1})),$$

where  $\Phi(u_{k-1}) := \mathbb{E}[U_k | u_{k-1}]$  and  $\Omega(u_{k-1}) := \text{Cov}[U_k | u_{k-1}]$  stand for the conditional mean and covariance of the SDE solution  $U$ , respectively. See, for example, [49] for how to do so.

Gaussian filters and smoothers approximate  $p(u_k | y_{1:k}) \approx \mathcal{N}(u_k | m_k, P_k)$ ,  $p(u_k | y_{1:T}) \approx \mathcal{N}(u_k | m_k^s, P_k^s)$ , and  $p(u_0) = \mathcal{N}(u_0 | m_0, P_0)$ . The Gaussian filter computes the filtering estimates  $\{m_k, P_k\}_{k=1}^T$  by

$$\begin{aligned} m_k^- &= \int \Phi(u_{k-1}) \mathcal{N}(u_{k-1} | m_{k-1}, P_{k-1}) du_{k-1}, \\ P_k^- &= \int (\Omega(u_{k-1}) + \Phi(u_{k-1}) \Phi(u_{k-1})^\top) \\ &\quad \times \mathcal{N}(u_{k-1} | m_{k-1}, P_{k-1}) du_{k-1} - m_k^- (m_k^-)^\top, \\ S_k &= H P_k^- H^\top + \Xi, \\ K_k &= P_k^- H^\top / S_k, \\ m_k &= m_k^- + K_k (y_k - H m_k^-), \\ P_k &= P_k^- - K_k S_k K_k^\top, \end{aligned}$$

for  $k = 1, 2, \dots, T$ . Define  $m_T^s := m_T$  and  $P_T^s := P_T$ . The Gaussian smoother computes the smoothing estimates  $\{m_k^s, P_k^s\}_{k=1}^{T-1}$  by

$$\begin{aligned} D_{k+1} &= \int u_k \Phi(u_k)^\top \mathcal{N}(u_k | m_k, P_k) du_k - m_k (m_{k+1}^-)^\top, \\ G_k &= D_{k+1} (P_{k+1}^-)^{-1}, \\ m_k^s &= m_k + G_k (m_{k+1}^s - m_{k+1}^-), \\ P_k^s &= P_k + G_k (P_{k+1}^s - P_{k+1}^-) G_k^\top, \end{aligned}$$

for  $k = T-1, T-2, \dots, 1$ . Depending on the application, we can use, for example, first-order Taylor expansion (i.e., EKFSs) or sigma-points (e.g., unscented transform) to approximate the integrals above. The approximate negative log-likelihood for optimising parameter  $\theta$  (i.e.,  $\lambda, b, \ell$ , and  $\sigma$ ) is given by

$$-\sum_{k=1}^T \log \mathcal{N}(y_k | H m_k^-, S_k; \theta). \quad (13)$$

The negative log-likelihood in Equation (13) depends on the parameters  $\theta$  through filtering recursions which in turn, are also complicated functions of the parameters. Deriving closed-form expressions for the gradients (or Hessian for that matter) as required for numerical optimisation is thus extremely challenging. Fortunately, however, it is also unnecessary because they can be computed efficiently using well-established techniques for automatic differentiation, as made available in a number of popular software libraries, such as JAX and TensorFlow.

### III. ERROR ANALYSIS

In this section, we analyse the estimation error that follows from using the chirp and IF estimation method introduced in Section II. Recall that this estimation method essentially solves a filtering and smoothing problem, and that we have a plethora of filters and smoothers to choose from. Therefore, we now narrow down our scope and focus on the particular, but useful Gaussian-based filter defined in Algorithm 1.

In literature, there already exists a number of studies on the stability of such filters [56–59]. However, these results are not always useful to this application because they assume that their state-space models are true. In other words, these classical results are not concerned with whether the state-space model is realistic or not. Thus, to take this into account, we analyse the estimation error when we feed the estimator with measurements from a true chirp signal and given an IF. Formally, the chirp measurement we consider is of the form

$$Y_k = \sin\left(2\pi \int_0^{t_k} f(s) ds\right) + \xi_k, \quad (14)$$

where  $f$  is the true given IF function that we want to estimate. When we input the measurement  $\{Y_1, Y_2, \dots, Y_k\}$  to the estimator, we would like to find a finite bound on the mean squared error

$$\mathbb{E}[|f(t_k) - g(H_V m_k)|^2],$$

where  $H_V$  is the operator that extracts  $V$ 's estimate from  $m_k$  (e.g.,  $H_V = [0 \ 0 \ 1 \ 0]$  when using the Matérn 3/2 prior). However, this is difficult to do due to the bijection  $g$  wrapping the estimates, therefore, we transform the analysis in the domain of the  $V$ 's. The mean squared error that we are interested in now becomes

$$\mathbb{E}[|g^{-1}(f_k) - H_V m_k|^2]. \quad (15)$$

In order to carry out the analysis, we also need to fix a representation of  $\Phi$  and  $\Omega$  in Algorithm 1. Thanks to the hierarchical structure of SDE (11), we can apply the ad-hoc locally conditional discretisation (LCD) [39, 60]. This LCD scheme approximates  $\Phi$  and  $\Omega$  by

$$\begin{aligned} \Phi(u_{k-1}) &= \text{blkdiag}\left(e^{-\Delta_k \lambda} \begin{bmatrix} \cos(\phi_{k-1}) & -\sin(\phi_{k-1}) \\ \sin(\phi_{k-1}) & \cos(\phi_{k-1}) \end{bmatrix}, e^{\Delta_k M}\right) u_{k-1}, \\ \Omega(u_{k-1}) &= \Omega_{k-1} = \text{blkdiag}(\Sigma(\Delta_k), \Lambda(\Delta_k)), \\ \phi_{k-1} &:= \Delta_k 2\pi g(H_V u_{k-1}), \\ \Delta_k &:= t_k - t_{k-1}. \end{aligned} \quad (16)$$

The exact formulae of  $e^{\Delta_k M}$  and  $\Lambda(\Delta_k)$  under the Matérn 3/2 case in Equation (10) are shown in Appendix A. It is worth noting again that the work in [26, 27] is a special case of Equation (16) under this particular discretisation scheme and parameter choice.

The main result (i.e., the error bound) is shown in Theorem 5. In order to obtain the result, we use the following assumptions.

**Assumption 2** (Regularity of IF and prior). *There exist a non-negative function  $z$  and constant  $c \geq 0$  such that at each  $k$ ,*

$$|g^{-1}(f_k) - \bar{H}_V e^{\Delta_k M} x|^2 \leq z(\Delta_k) |g^{-1}(f_{k-1}) - \bar{H}_V x|^2 + c$$

for all  $x \in \mathbb{R}^{d_v}$ , where  $\bar{H}_V \in \mathbb{R}^{d_v}$  is defined in Section II-B.

Assumption 2 confines the class of IF functions and bijections that this error analysis is dealing with. Essentially, this assumption means that for any pair of  $(x, g^{-1}(f_{k-1}))$  at  $t_{k-1}$ , the error (between  $x$  and the true IF value  $g^{-1}(f_{k-1})$ ) should not grow significantly (controlled by  $z$  and  $c_k$ ) to time  $t_k$  when the prior makes a prediction based on  $x$ . This makes sense because one must choose the prior for IF appropriately in order to best describe the latent IF. Note that we also have the freedom to choose a positive bijection  $g$  to satisfy this assumption.

To see that Assumption 2 is not restrictive, we can enumerate a few realistic examples that satisfy the assumption. Suppose that the true IF is  $f(t) = \sin(t) + \epsilon$  for some base frequency  $\epsilon > 1$ , and that we choose  $g(\cdot) = \exp(\cdot)$  and  $M = -1$  (i.e., a  $d_v = 1$  Matérn 1/2 prior). Then there exists a constant  $c$  (independent of both  $k$  and  $\Delta_k$ ) and a function  $z(\Delta_k) = e^{\Delta_k M}$  that satisfy this assumption. Moreover, it is not hard to manipulate  $\Delta_k$  or  $M$  so that  $z(\Delta_k) < 1/3$  in order to obtain a contractive error bound as in Corollary 6.

**Assumption 3.** *There exist constants  $c_P$  and  $c_{\bar{P}}$  such that  $\text{tr}(P_k) \leq c_P$  and  $\|P_k^-\|_2^2 \leq c_{\bar{P}}$  almost surely for all  $k \geq 1$ .*

Assumption 3 requires that the filtering and prediction covariances are finitely bounded. This assumption is indeed strong, in the sense that it is hard to verify in practice. On the other hand, relaxing this assumption is difficult because the evolution of these covariances is non-linearly coupled with that of the posterior mean estimates and measurements, while the evolution of the posterior mean estimates depends on the covariances too. This is a common problem in analysing the stability of non-linear filters, and this type of assumptions is regularly used in the literature [59].

**Lemma 4.** *For any mean  $\mu \in \mathbb{R}^{d_u}$  and covariance  $\Theta \in \mathbb{R}^{d_u \times d_u}$ , the conditional mean  $\Phi$  is such that*

$$\int \|\Phi(u)\|_2^2 N(u | \mu, \Theta) du \leq \|\mu\|_2^2 + \text{tr}(\Theta). \quad (17)$$

*Proof.* This follows from the fact that  $\|\Phi(u)\|_2 \leq \|u\|_2$  for all  $u \in \mathbb{R}^{d_u}$  in Equation (16).  $\square$

**Theorem 5.** *Suppose that Assumptions 2 and 3 hold. Then for every  $k \geq 1$ , the error is such that*

$$\begin{aligned} & \mathbb{E}[|g^{-1}(f_k) - H_V m_k|^2] \\ & \leq e_0 \prod_{j=1}^k 3z(\Delta_j) + \gamma \sum_{j=1}^k \prod_{i=1}^{j-1} 3z(\Delta_{k-i+1}) \\ & \quad + \sum_{j=1}^k \zeta_{k-j+1} \prod_{i=1}^{j-1} 3z(\Delta_{k-i+1}), \end{aligned} \quad (18)$$

where  $e_0 := \mathbb{E}[|g^{-1}(f_0) - H_V m_0|^2]$  stands for the initial error, and

$$\begin{aligned} \gamma &:= 3c + \frac{6c_{\bar{P}}}{(c_{\Sigma} + \Xi)^2}, \\ \zeta_k &:= (2c_K)^k \frac{3c_{\bar{P}}(\|m_0\|_2^2 + \text{tr}(P_0))}{(c_{\Sigma} + \Xi)^2} \\ & \quad + \frac{3c_{\bar{P}}}{(c_{\Sigma} + \Xi)^2} \left( 2 \frac{c_{\bar{P}}(1 + \Xi)}{(c_{\Sigma} + \Xi)^2} + c_P \right) \sum_{j=0}^{k-1} (2c_K)^j, \\ c_{\Sigma} &:= \inf_{j \geq 1} \Sigma(\Delta_j). \end{aligned} \quad (19)$$

Note that we define  $\prod_{i=1}^0 := 1$  and  $\sum_{j=0}^0 := 0$ .

*Proof.* Thanks to Assumption 3, the Kalman gain is such that

$$\|K_k\|_2^2 = \|P_k^- H^T / S_k\|_2^2 \leq \frac{c_{\bar{P}}}{(c_{\Sigma} + \Xi)^2}$$

then  $\|I - K_k H\|_2^2 \leq c_K$  for some constant  $c_K$  (determined by  $c_{\bar{P}}$ ,  $c_{\Sigma}$ , and  $\Xi$ ), almost surely.

By applying the triangle inequality on the mean squared error, we arrive at a bound composed of three residuals:

$$\begin{aligned} & \mathbb{E}[|g^{-1}(f_k) - H_V m_k|^2] \\ & = \mathbb{E}[|g^{-1}(f_k) - H_V m_k^- + H_V K_k (Y_k - H m_k^-)|^2] \quad (20) \\ & \leq 3 \mathbb{E}[|g^{-1}(f_k) - H_V m_k^-|^2] \\ & \quad + 3 \mathbb{E}\left[\left|H_V K_k \left(\sin\left(\int_0^{t_k} 2\pi f(s) ds\right) - H m_k^-\right)\right|^2\right] \\ & \quad + 3 \mathbb{E}[|H_V K_k \xi_k|^2]. \end{aligned}$$

The last residual satisfies  $\mathbb{E}[|H_V K_k \xi_k|^2] \leq c_{\bar{P}} / (c_{\Sigma} + \Xi)^2$ . We can establish a bound to the first residual by applying Assumption 2, hence, we have

$$\begin{aligned} & \mathbb{E}[|g^{-1}(f_k) - H_V m_k^-|^2] \\ & \leq z(\Delta_k) \mathbb{E}[|g^{-1}(f_{k-1}) - H_V m_{k-1}^-|^2] + c. \end{aligned}$$

As for the second residual, we have

$$\begin{aligned} & \mathbb{E}\left[\left|H_V K_k \left(\sin\left(\int_0^{t_k} 2\pi f(s) ds\right) - H m_k^-\right)\right|^2\right] \\ & \leq \frac{c_{\bar{P}}}{(c_{\Sigma} + \Xi)^2} \mathbb{E}\left[\left|\sin\left(\int_0^{t_k} 2\pi f(s) ds\right) - H m_k^-\right|^2\right] \quad (21) \\ & \leq \frac{c_{\bar{P}}(1 + \mathbb{E}[\|m_k^-\|_2^2])}{(c_{\Sigma} + \Xi)^2}. \end{aligned}$$

Lemma 4 and Assumption 3 imply that

$$\begin{aligned} \mathbb{E}[\|m_k^-\|_2^2] & \leq \mathbb{E}[\|m_{k-1}\|_2^2 + \text{tr}(P_{k-1})] \\ & \leq 2 \mathbb{E}[\|(I - K_{k-1} H) m_{k-1}^-\|_2^2] \\ & \quad + 2 \mathbb{E}[\|K_{k-1} Y_{k-1}\|_2^2] + c_P \quad (22) \\ & \leq 2c_K \mathbb{E}[\|m_{k-1}^-\|_2^2] + 2 \frac{c_{\bar{P}}(1 + \Xi)}{(c_{\Sigma} + \Xi)^2} + c_P. \end{aligned}$$

By unrolling the recursion of  $\mathbb{E}[\|m_k^-\|_2^2]$  from the equation above for  $k \geq 1$ , we obtain

$$\begin{aligned} \mathbb{E}[\|m_k^-\|_2^2] & \leq (2c_K)^k (\|m_0\|_2^2 + \text{tr}(P_0)) \\ & \quad + \left( 2 \frac{c_{\bar{P}}(1 + \Xi)}{(c_{\Sigma} + \Xi)^2} + c_P \right) \sum_{j=0}^{k-1} (2c_K)^j, \end{aligned} \quad (23)$$



noting that the initial  $\mathbb{E}[\|m_1^-\|_2^2] = \|m_1^-\|_2^2 \leq \|m_0\|_2^2 + \text{tr}(P_0)$ . Equation (23) can then be substituted back into Equation (21). Therefore, by putting it all together, we have

$$\begin{aligned} & \mathbb{E}[|g^{-1}(f_k) - H_V m_k|^2] \\ & \leq 3z(\Delta_k) \mathbb{E}[|g^{-1}(f_{k-1}) - H_V m_{k-1}|^2] + 3c \\ & \quad + \frac{3c_P}{(c_\Sigma + \Xi)^2} + (2c_K)^k \frac{3c_P(\|m_0\|_2^2 + \text{tr}(P_0))}{(c_\Sigma + \Xi)^2} \\ & \quad + \frac{3c_P}{(c_\Sigma + \Xi)^2} \left( 2 \frac{c_P(1 + \Xi)}{(c_\Sigma + \Xi)^2} + c_P \right) \sum_{j=0}^{k-1} (2c_K)^j \\ & \quad + 3 \frac{c_P}{(c_\Sigma + \Xi)^2} \end{aligned} \quad (24)$$

which is a recursion of the error. Unrolling the recursion for  $k \geq 1$  concludes the result.  $\square$

Theorem 5 provides an upper bound of the estimation error in the mean square sense. This bound is dominated by the function  $z$  and the constant  $c_K$ , in the way that the bound is contractive as long as  $z$  and  $c_K$  are not too large. This result makes sense because it reflects that the IF prior should be chosen well enough to model the true IF (see Assumption 2), and that the Kalman gain should be non-explosive too.

In the following corollary, we show that the error bound from Theorem 5 can be simplified to a contractive one when  $z$  and  $c_K$  meet a certain criterion.

**Corollary 6.** *Following Theorem 5, suppose that  $c_K < 1/2$ , and that  $z(\Delta_j) \leq c_z < 1/3$  for all  $j = 1, 2, \dots, k$ , then the error bound in Equation (18) reduces to*

$$\mathbb{E}[|g^{-1}(f_k) - H_V m_k|^2] \leq (3c_z)^k e_0 + \frac{\gamma + \bar{\zeta}}{1 - 3c_z}, \quad (25)$$

where

$$\bar{\zeta} := \frac{3c_P}{(c_\Sigma + \Xi)^2} \left( \|m_0\|_2^2 + \text{tr}(P_0) + \frac{2c_P(1 + \Xi)}{(c_\Sigma + \Xi)^2} + c_P \right).$$

*Proof.* Recall the identity that  $\sum_{j=0}^k a^j < \frac{1}{1-a}$  for every number  $0 < a < 1$  and indexes  $k = 0, 1, \dots$ . By applying the assumptions and this identity to Equation (18) we conclude the result.  $\square$

It is worth noting that the error bound in the main theorem does not reflect how well the chirp prior cope with the chirp signal. Indeed, the bound shows that the prior for the IF should be well chosen through  $z$ , but it does not explicitly reveal how well the harmonic SDE (6) model the chirp signal in Equation (14). This is due to Equation (20) where we used a worst-case triangle bound on the residual between the chirp prediction (i.e.,  $H m_k^-$ ) and the true chirp signal (i.e.,  $\sin(\int_0^{t_k} 2\pi f(s) ds)$ ): they are both bounded. Eventually, this residual error is not directly reflected in the final error bound but it is instead implicitly contained in that of the constant  $c_K$ . We believe that the error bound can be improved if we can obtain a better bound on the chirp residual. This is a worthwhile future work.

Table I  
MEANS AND STANDARD DEVIATIONS (FROM 100 MC RUNS) OF IF ESTIMATION RMSES OVER COMBINATIONS OF ESTIMATION METHODS AND CHIRP SIGNALS. METHODS BELOW THE DASH LINE ARE THE PROPOSED ONES IN THIS PAPER. BOLD NUMBERS REPRESENT THE BEST IN EACH OF THEIR COLUMNS. DETAILED STATISTICS OF THE RMSES ARE FOUND IN FIGURE 6.

RMSE ( $\times 10^{-1}$ )	$\alpha(t) = 1$	$\alpha(t) = e^{-0.3t}$	$\alpha(t)$ is a random process
Hilbert transform	$7.13 \pm 2.35$	$11.74 \pm 11.06$	$54.63 \pm 25.58$
Spectrogram	$1.53 \pm 0.08$	$1.82 \pm 0.18$	$8.17 \pm 4.31$
Polynomial MLE	$8.87 \pm 0.09$	$8.90 \pm 0.13$	$10.01 \pm 4.33$
ANF	$2.13 \pm 0.16$	$3.05 \pm 0.31$	$37.77 \pm 23.57$
EKFS MLE on (2)	$1.09 \pm 0.20$	$19.53 \pm 18.14$	$41.46 \pm 19.48$
GHFS MLE on (2)	$0.67 \pm 0.17$	$3.84 \pm 7.95$	$39.47 \pm 19.36^\dagger$
EKFS MLE	$0.70 \pm 0.17$	$0.98 \pm 0.24$	$6.37 \pm 7.04$
GHFS MLE	<b><math>0.65 \pm 0.16</math></b>	<b><math>0.93 \pm 0.24</math></b>	$5.36 \pm 5.59$
CD-EKFS MLE	$1.53 \pm 0.67$	$2.86 \pm 2.26$	$6.05 \pm 6.55$
CD-GHFS MLE	$0.72 \pm 0.18$	$1.16 \pm 0.34$	<b><math>4.91 \pm 3.74^\ddagger</math></b>

$^\dagger$  and  $^\ddagger$  encounter 1 and 15 NaN numerical errors, respectively.

Table II  
ESTIMATED MODEL PARAMETERS FROM THE GHFS MLE METHOD SHOWN IN FIGURE 4. THE PARAMETER  $\lambda$  IN THE SECOND COLUMN IS BOLD BECAUSE ITS ESTIMATE IS VERY CLOSE TO THE TRUE DAMPING FACTOR 0.3.

	$\alpha(t) = 1$	$\alpha(t) = e^{-0.3t}$	$\alpha(t)$ is a random process
$\lambda$	$2.06 \times 10^{-2}$	<b><math>3.00 \times 10^{-1}</math></b>	1.05
$b$	$8.07 \times 10^{-5}$	$5.77 \times 10^{-3}$	1.05
$\delta$	$4.51 \times 10^{-1}$	$4.56 \times 10^{-1}$	$0.99 \times 10^{-1}$
$\ell$	1.20	1.14	1.33
$\sigma$	4.88	4.86	5.98
$m_0^V$	10.37	10.26	12.97

## IV. EXPERIMENTS

In this section, we test the performance of the proposed chirp IF estimation scheme on a synthetic model, and a real application that is concerned with gravitational wave frequency estimation. Furthermore, for the sake of reproducibility, their implementations are published at address <https://github.com/spdes/chirpgp>.

### A. Synthetic experiment

The synthetic model that we use to test the performance is given in the following equations.

$$f(t) = a b \cot(t) \csc(t) e^{-b \csc(t)} + c, \quad t \in (0, \pi),$$

$$Y_k = \alpha(t_k) \sin\left(2\pi \int_0^{t_k} f(s) ds\right) + \xi_k, \quad \xi_k \sim \mathcal{N}(0, 0.1),$$

where  $f$  is the true IF parametrised by  $a = 500$ ,  $b = 5$ , and  $c = 8$  (which control the function's amplitude, horizontal scale, and offset, respectively). The chirp signal is generated as per  $f(t)$ 's phase  $a \exp(-b/\sin(t)) + ct$  and amplitude  $\alpha(t)$ . Measurements of this chirp signal at any time  $t_k$  is represented by a random variable  $Y_k$  along with a Gaussian noise  $\xi_k$ .

In order to test IF estimation methods against the nuisance from chirp amplitude (i.e., estimation methods do not know the form of  $\alpha$ ), we consider three choices of  $\alpha$ , that are, constant  $\alpha(t) = 1$ , damped  $\alpha(t) = \exp(-0.3t)$ , and a



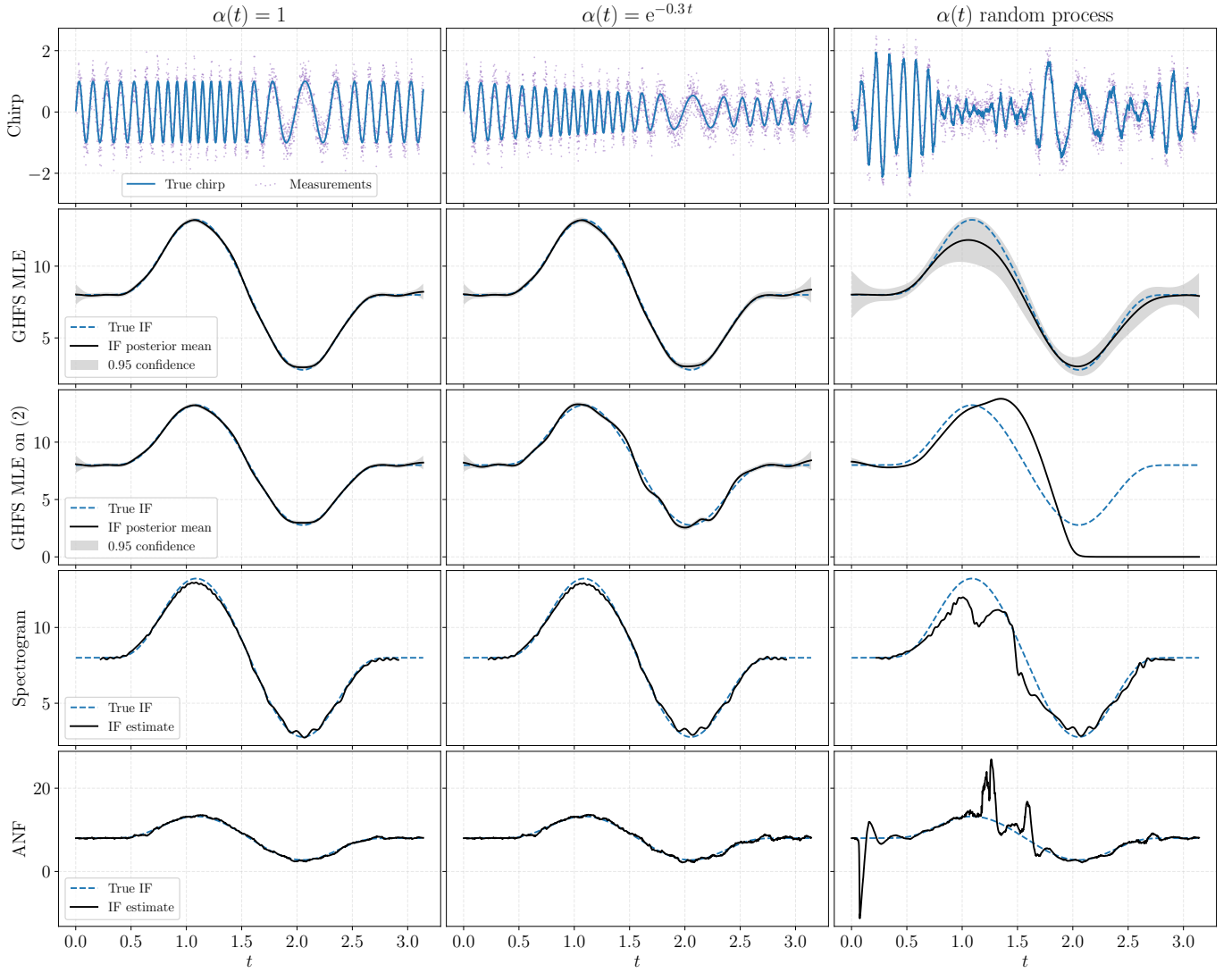


Figure 4. IF estimates from one MC run. For the sake of demonstration simplicity, only four methods are shown.

random  $\alpha$ . More specifically, the random  $\alpha(t)$  is generated from an Ornstein–Uhlenbeck SDE  $d\alpha(t) = -\alpha(t)dt + dW(t)$ . This randomised amplitude sets significant challenges for IF estimation methods.

The true chip signal and measurements from this synthetic model are generated in the time interval  $(0, \pi)$  under sampling frequency 1,000 Hz (i.e., 3,141 data points in total). The estimation performance is quantified by the root mean squared error (RMSE). Furthermore, we run all the IF estimation methods using 100 independent Monte Carlo (MC) simulations in order to get a statistic of their RMSE results. In these MC runs, measurement noises  $\xi$  and random amplitude  $\alpha$  are generated using independent random seeds.

We apply the extended Kalman filter and smoother (EKFS) and 3rd-order Gauss–Hermite Gaussian filter and smoother (GHFS) – which are the most popular realisations of Algorithm 1 – to solve the proposed model in Equation (11). The discretisation of this model is performed using the LCD scheme in Equation (16) and bijection  $g(\cdot) = \log(\exp(\cdot) + 1)$ . In addition, since our model can be solved in continuous-time,

we also apply the continuous-discrete EKFS and GHKF (CD-EKFS and CD-GHFS) [53] to solve it directly without using any SDE discretisation.

The proposed model in Equation (11) consists of six parameters, that are,  $\lambda$ ,  $b$ ,  $\delta$ ,  $\ell$ ,  $\sigma$ , and the initial mean of  $V$  denoted  $m_0^V$ . They are determined via maximum likelihood estimation (MLE) by minimising the objective function in Equation (13) with the L-BFGS [61] optimiser.

We consider the following baseline methods to compare with ours: the Hilbert transform, first-order power spectrum (spectrogram), adaptive notch filter (ANF) [35], 10-th order polynomial regression, and the state-space method by [25–27]. In particular, this mentioned state-space method is arguably the most interesting to compare with, as it uses a model (cf. Equation (2)) that is a special case of ours (see Section II-C). We solve their state-space models by using the same EKFS and GHFS, and mark them as “EKFS/GHFS on (2)” in the result figure/table. The parameters and settings of these baseline methods are detailed in Appendix B.

RMSE results are summarised in Table I along with a

detailed statistical boxplot in Figure 6. From the table and figure, it is clear that the IF estimation methods that are based on the proposed model outperform all other methods (in terms of mean, median, quantiles, and minimum). In particular, when the amplitude function  $\alpha$  is a random process, the proposed methods are significantly better than others. This verifies that the proposed model is amenable for tackling amplitude nuisances to a good extent, thanks to modelling chirp as a GP. When the amplitude is a constant, however, the margin of using the proposed model over that of Equation (2) is not significant. Among all the state-space based methods, GHFS produce slightly better results than EKFS.

The IF estimates from one MC run are plotted in Figure 4. This figure qualitatively shows that the GHFS MLE method provides the best IF estimates compared to other three methods. Furthermore, from the figure in the second row and third column, we can see that the confidence interval (CI) produced by GHFS MLE is reasonable: the true IF always lies within the CI; Moreover, we can also see that the CI at  $t \approx 0.5$  is increasing until  $t \approx 1.2$ , while at the same time, the error between the mean estimate and true IF is increasing as well. Similarly, the CI decreases as the error decreases around  $t \in [1.2, 2.0]$ . In contrast, the figure in the third row and third column shows that the method “GHFS MLE on (2)” gives erroneous and overconfident estimates. This is because the underlying model in Equation (2) does not take chirp randomness into account.

Table II shows the estimated model parameters by the GHFS MLE method from the same MC run plotted in Figure 4. We found that these estimated parameters are meaningful, especially for  $\lambda$  and  $b$  which determine the chirp prior’s damping factor and stochastic volatility, respectively. When  $\alpha$  is a constant,  $\lambda$  and  $b$  are estimated to have small values because the true chirp has no damping nor randomness. When  $\alpha(t) = e^{-0.3t}$ , the estimated  $\lambda \approx 0.3$  is very close to the true damping value. When  $\alpha$  is random,  $b$  is no longer estimated to be small so as to account for the stochastic volatility of this randomised chirp. As for  $V$ ’s parameters  $\ell$  and  $\sigma$ , their estimated values do not change significantly with different forms of  $\alpha$ . This result is desired because the chirp amplitude  $\alpha$  does not affect the chirp IF.

### B. Gravitational wave frequency estimation

We use the proposed model to estimate the frequency of a gravitational wave (GW) signal. The GW signal is taken from a well-known binary black hole collision event GW150914 in 2016 [62]. This signal is evenly sampled at 16,384 Hz and contains 3,441 measurements. More details regarding this data can be found in [62]. To estimate the chirp and frequency from the GW measurements, we use the same GHFS MLE method as in the synthetic experiment, which has the best RMSE statistic.

The GW chirp and frequency estimation result is shown in Figure 5. From this figure, we can see that the frequency slowly increases from around 50 Hz at  $t \approx 0.35$  s to 80 Hz at  $t \approx 0.4$  s. Then, starting from  $t \approx 0.4$  s, the frequency sharply increases to around 250 Hz until  $t \approx 4.3$  s, followed

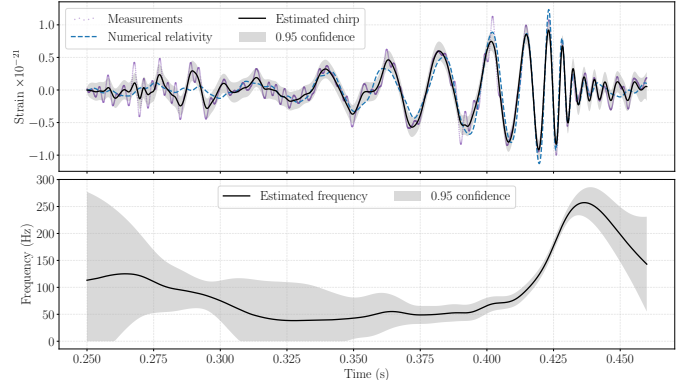


Figure 5. Gravitational wave frequency (and chirp) estimation by using the GHFS MLE method on the model in Equation (11). Estimated model parameters are  $\lambda = 1.59 \times 10^1$ ,  $b = 2.12$ ,  $\delta = 7.78 \times 10^{-15}$ ,  $\ell = 4.21 \times 10^{-2}$ ,  $\sigma = 1.30 \times 10^2$ , and  $m_0^V = 3.91 \times 10^{-4}$ .

by a sharp decrease from  $t \geq 4.3$ . This estimation result makes sense, as it follows the theoretical prediction from the GW model of merging binary black hole [62]. Moreover, the estimated frequency is close to that of the one shown in [62, Fig. 1, left bottom]. The confidence interval indicates that the estimator is confident around the region  $t \in [0.4, 0.43]$  which is the most interesting section.

## V. CONCLUSIONS

In this paper, we have designed a hierarchical Gaussian process prior for jointly modelling chirp signal and its instantaneous frequency (IF). This enables us to estimate a wide class of chirp signals and their IFs in continuous-time and probabilistic (posterior) distribution. In order to carry out the estimation/computation in practice, we realise this prior model in a non-linear stochastic differential equation, and solve the posterior distribution by using stochastic filtering and smoothing methods (e.g., sigma-points filters and smoothers). Moreover, model parameters, which control the characteristics of the chirp and IF, can be determined via maximum likelihood estimation and auto-differentiation. Theoretical analysis shows that this model results in a bounded mean squared error for a class of state-space solvers and chirp signals. Experiment results show that the proposed model significantly outperforms a number of baseline methods, and is applicable to real data (e.g., gravitational wave) as well.

Lastly, it is worth saying a few words about the plausibility of the model and possible future works. Currently, the chirp is assumed to consist of a single time-varying sinusoidal. However, the present methodology could be extended to harmonic chirps [19, 63] by replacing the single-harmonic model in Equation (6) with a multi-harmonic period GP model similarly to [48, 64] and by estimating the parameters of the resulting hierarchical GP model. Instead of estimating the parameters, a known harmonic structure of the harmonic chirp could also be encoded into the parameters of the models of the harmonics. In the resulting model the latent GP for the IF is shared among the single-harmonic SDE components as their frequencies can be assumed to be integer multiples of the base IF. Conditionally to the IF trajectory, the model is still linear

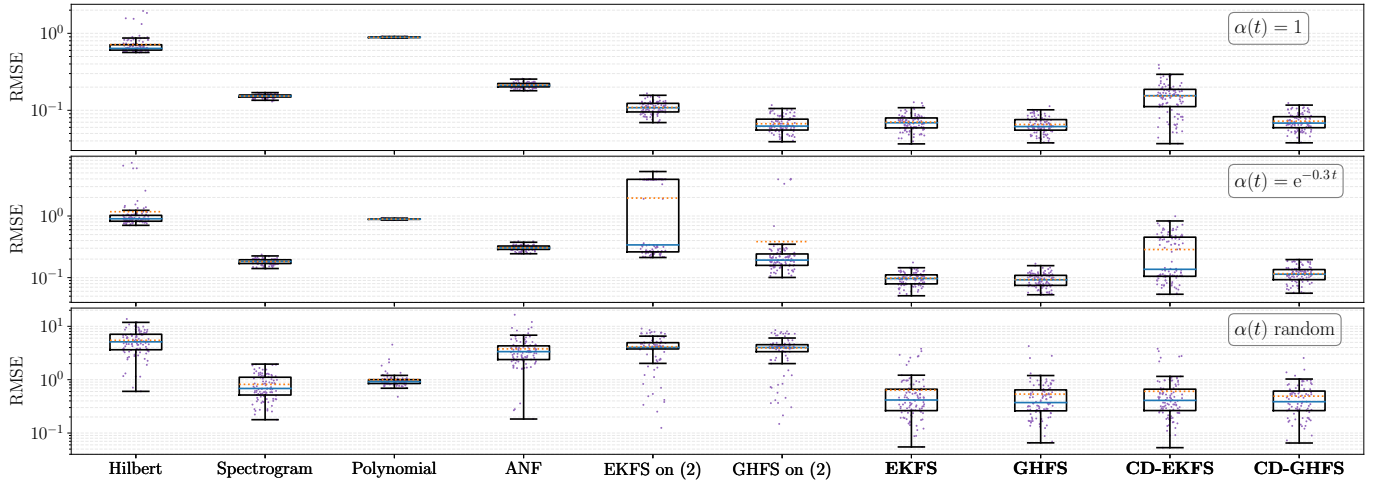


Figure 6. Boxplot (in log-scale) of IF estimation RMSEs. Purple scattered points stand for the RMSEs in each of their methods' 100 MC runs, summarised by boxes and whiskers that represent the first-third quantiles and 1.5 interquartile range, respectively. The blue solid and orange dotted lines indicate the median and mean of the RMSEs, respectively. Methods in bold font are the proposed ones in this paper. Compared to Table I, the word “MLE” is omitted in order to save space.

Gaussian. Therefore similar Gaussian filters and smoothers as in Algorithm 1 are still applicable.

The proposed model could also be extended to cover superimposed chirps [65] by assuming two or more different frequencies and modelling the measurements as a superposition of independent (possibly harmonic) chirps with different IFs. However, state and parameter estimation in the resulting model can be expected to be much harder than in single-frequency case due to symmetry arising from exchangeability of the frequencies between the different chirp signals.

The assumption of whiteness and Gaussianity of the measurement noise can also be relaxed. Correlations in the measurement noise can result from, for instance, wind hitting the microphones which causes non-white disturbance to the signal. These correlations can be modelled by replacing or augmenting the measurement noise with an additional state-component which is modelled as a coloured process [66]. As this retains the conditional Gaussian structure of the model, the Gaussian filters and smoothers can still be expected to be applicable. Non-Gaussianity of the noise is often due to outliers arising from shot-noises in the signals which can be modelled, for example, by replacing the Gaussian noise with a Student's t-noise. For filtering and smoothing methods for this kind of models, see, for example, [67–70].

#### APPENDIX A

In Equation (16), the explicit discretisation of the Matérn 3/2 SDE are given in the following equations.

$$e^{\Delta_k M} = e^{-\Delta_k \gamma} \begin{bmatrix} 1 + \Delta_k \gamma & \Delta_k \\ -\Delta_k \gamma^2 & 1 - \Delta_k \gamma \end{bmatrix},$$

$$\begin{aligned} \Lambda(\Delta_k) &:= \int_0^{\Delta_k} e^{(\Delta_k-s)M} N N^T (e^{(\Delta_k-s)M})^T ds \\ &= \begin{bmatrix} \sigma^2 - \beta(2\eta + 2\eta^2 + 1) & 2\Delta_k^2 \gamma^3 \beta \\ 2\Delta_k^2 \gamma^3 \beta & \gamma^2(\sigma^2 + \beta(2\eta - 2\eta^2 - 1)) \end{bmatrix}, \end{aligned}$$

where  $\gamma := \sqrt{3}/\ell$ ,  $\beta := \sigma^2 \exp(-2\eta)$ , and  $\eta := \Delta_k \gamma$ .

#### APPENDIX B

Parameters and settings of the baseline methods in Section IV-A are given as follows.

- The Hilbert transform method uses a cascaded second-order forward-backward digital filter to preprocess the noisy measurements. The filter uses an 8-th order Butterworth design with 18 Hz critical frequency.
- The spectrogram method uses the same filtering procedure as in the Hilbert transform method to preprocess measurements. We choose the cosine time window with 450 length and 449 overlaps.
- The (pilot) adaptive notch filter is from [35, Table II]. Its parameters ( $\mu = 0.015$ ,  $\gamma_w = \mu^2/2$ , and  $\gamma_\alpha = \mu \gamma_w/4$  under [35]'s notation) are selected as per the guidance in [35, pp. 2032].
- The polynomial method fits the IF by a 10-th order polynomial, the coefficients of which are determined via maximum likelihood estimation and Levenberg–Marquardt optimisation.

#### REFERENCES

- [1] B. Boashash, “Estimating and interpreting the instantaneous frequency of a signal — Part 1: Fundamentals,” *Proceedings of the IEEE*, vol. 80, no. 4, pp. 520–538, 1992.
- [2] —, “Estimating and interpreting the instantaneous frequency of a signal — Part 2: Algorithms and applications,” *Proceedings of the IEEE*, vol. 80, no. 4, pp. 540–568, 1992.
- [3] R. J. Fitzgerald, “Effects of range-Doppler coupling on chirp radar tracking accuracy,” *IEEE Transactions on Aerospace and Electronic Systems*, vol. 10, no. 4, pp. 528–532, 1974.
- [4] B. Reynders and S. Pollin, “Chirp spread spectrum as a modulation technique for long range communication,” in *Proceedings of the 2016 Symposium on Communications and Vehicular Technologies (SCVT)*, 2016, pp. 1–5.

- [5] T. Collins and P. Atkins, "Nonlinear frequency modulation chirps for active sonar," *IEEE Proceedings - Radar, Sonar and Navigation*, vol. 146, no. 6, pp. 312–316, 1999.
- [6] S. Fomel, "Local seismic attributes," *Geophysics*, vol. 72, no. 3, pp. 29–33, 2007.
- [7] G. Liu, S. Fomel, and X. Chen, "Time-frequency analysis of seismic data using local attributes," *Geophysics*, vol. 76, no. 6, pp. 23–34, 2011.
- [8] M. Maggiore, *Gravitational Waves: Volume 1: Theory and Experiments*. Oxford University Press, 2008.
- [9] O. Besson, M. Ghogho, and A. Swami, "Parameter estimation for random amplitude chirp signals," *IEEE Transactions on Signal Processing*, vol. 47, no. 12, pp. 3208–3219, 1999.
- [10] X. Meng, A. Jakobsson, X. Li, and Y. Lei, "Estimation of chirp signals with time-varying amplitudes," *Signal Processing*, vol. 147, pp. 1–10, 2018.
- [11] Y. Doweck, A. Amar, and I. Cohen, "Fundamental initial frequency and frequency rate estimation of random-amplitude harmonic chirps," *IEEE Transactions on Signal Processing*, vol. 63, no. 23, pp. 6213–6228, 2015.
- [12] D. Gabor, "Theory of communication," *Journal of the Institution of Electrical Engineers*, vol. 93, no. 26, pp. 429–457, 1946.
- [13] T. J. Abatzoglou, "Fast maximum likelihood joint estimation of frequency and frequency rate," *IEEE Transactions on Aerospace and Electronic Systems*, vol. 22, no. 6, pp. 708–715, 1986.
- [14] P. M. Djurić and S. M. Kay, "Parameter estimation of chirp signals," *IEEE Transactions on Acoustics, Speech, and Signal Processing*, vol. 38, no. 12, pp. 2118–2126, 1990.
- [15] S. Peleg and B. Porat, "Linear FM signal parameter estimation from discrete-time observations," *IEEE Transactions on Aerospace and Electronic Systems*, vol. 27, no. 4, pp. 607–616, 1991.
- [16] X.-G. Xia, "Discrete chirp-Fourier transform and its application to chirp rate estimation," *IEEE Transactions on Signal Processing*, vol. 48, no. 1, pp. 3122–3133, 2000.
- [17] B. Völcker and B. Ottersten, "Chirp parameter estimation from a sample covariance matrix," *IEEE Transactions on Signal Processing*, vol. 49, no. 3, pp. 603–612, 2001.
- [18] P. O'Shea, "A fast algorithm for estimating the parameters of a quadratic FM signal," *IEEE Transactions on Signal Processing*, vol. 52, no. 2, pp. 385–393, 2004.
- [19] J. Swärd, J. Brynolfsson, A. Jakobsson, and M. Hansson-Sandsten, "Sparse semi-parametric estimation of harmonic chirp signals," *IEEE Transactions on Signal Processing*, vol. 64, no. 7, pp. 1798–1807, 2016.
- [20] J. Kitchen, "A method for estimating the coefficients of a polynomial phase signal," *Signal Processing*, vol. 37, no. 3, pp. 463–470, 1994.
- [21] S. Peleg and B. Friedlander, "The discrete polynomial-phase transform," *IEEE Transactions on Signal Processing*, vol. 43, no. 8, pp. 1901–1914, 1995.
- [22] G. Zhou, G. B. Giannakis, and A. Swami, "On polynomial phase signals with time-varying amplitudes," *IEEE Transactions on Signal Processing*, vol. 44, no. 4, pp. 848–861, 1996.
- [23] M. L. Farquharson, "Estimating the parameters of polynomial phase signals," Ph.D. dissertation, Queensland University of Technology, 2006.
- [24] R. G. McKilliam, B. G. Quinn, I. V. L. Clarkson, B. Moran, and B. N. Vellambi, "Polynomial phase estimation by least squares phase unwrapping," *IEEE Transactions on Signal Processing*, vol. 62, no. 8, pp. 1962–1975, 2014.
- [25] D. L. Snyder, "The state-variable approach to analog communication theory," *IEEE Transactions on Information Theory*, vol. 14, no. 1, pp. 94–104, 1968.
- [26] B. F. La Scala, R. R. Bitmead, and M. R. James, "Conditions for stability of the extended Kalman filter and their application to the frequency tracking problem," *Mathematics of Control, Signals, and Systems*, vol. 8, no. 1, pp. 1–26, 1995.
- [27] B. F. La Scala and R. R. Bitmead, "Design of an extended Kalman filter frequency tracker," *IEEE Transactions on Signal Processing*, vol. 44, no. 3, pp. 739–742, 1996.
- [28] S. Bittanti and S. M. Savaresi, "On the parameterization and design of an extended Kalman filter frequency tracker," *IEEE Transactions on Automatic Control*, vol. 45, no. 9, pp. 1718–1724, 2000.
- [29] J. Gál, A. Câmpăanu, and I. Naforntă, "The estimation of chirp signals parameters by an extended Kalman filtering algorithm," in *Proceedings of International Symposium on Signals, Circuits and Systems*, 2011, pp. 1–4.
- [30] A. Routray, A. K. Pradhan, and K. P. Rao, "A novel Kalman filter for frequency estimation of distorted signals in power systems," *IEEE Transactions on Instrumentation and Measurement*, vol. 51, no. 3, pp. 469–479, 2002.
- [31] A. Dardanelli, S. Corbetta, I. Boniolo, S. M. Savaresi, and S. Bittanti, "Model-based Kalman filtering approaches for frequency tracking," in *IFAC Proceedings Volumes*, vol. 43, 2010, pp. 37–42.
- [32] C. Dubois, M. Davy, and J. Idier, "Tracking of time-frequency components using particle filtering," in *Proceedings of International Conference on Acoustics, Speech, and Signal Processing*, vol. 4, 2005, pp. 9–12.
- [33] E. E. Tsakonas, N. D. Sidiropoulos, and A. Swami, "Optimal particle filters for tracking a time-varying harmonic or chirp signal," *IEEE Transactions on Signal Processing*, vol. 56, no. 10, pp. 4598–4610, 2008.
- [34] P. K. S. Tam and J. B. Moore, "A Gaussian sum approach to phase and frequency estimation," *IEEE Transactions on Communications*, vol. 25, no. 9, pp. 935–942, 1977.
- [35] M. Niedźwiecki and M. Meller, "New algorithm for adaptive notch smoothing," *IEEE Transactions on Signal Processing*, vol. 59, no. 5, pp. 2024–2037, 2011.
- [36] M. Meller, "Automatic optimization of adaptive notch filter's frequency tracking," in *Proceedings of the 22nd European Signal Processing Conference*, 2014, pp. 431–435.
- [37] C. E. Rasmussen and C. K. I. Williams, *Gaussian Processes for Machine Learning*. The MIT Press, 2006.
- [38] Z. Zhao, M. Emzir, and S. Särkkä, "Deep state-space Gaussian processes," *Statistics and Computing*, vol. 31, no. 6, p. 75, 2021.
- [39] Z. Zhao, "State-space deep Gaussian processes with applications," Ph.D. dissertation, Aalto University, 2021.
- [40] D. J. C. MacKay, "Introduction to Gaussian processes," in *Neural Networks and Machine Learning*, ser. NATO ASI Series F Computer and Systems Sciences, 1998, vol. 168, pp. 133–166.
- [41] E. Snelson and Z. Ghahramani, "Sparse Gaussian processes using pseudo-inputs," in *Proceedings of Advances in Neural Information Processing Systems 18*. MIT Press, 2006, pp. 1257–1264.
- [42] J. Quiñero-Candela and C. E. Rasmussen, "A unifying view of sparse approximate Gaussian process regression," *Journal of Machine Learning Research*, vol. 6, pp. 1939–1959, 2005.
- [43] M. Titsias, "Variational learning of inducing variables in sparse Gaussian processes," in *Proceedings of the 12th International Conference on Artificial Intelligence and Statistics*, vol. 5. PMLR, 2009, pp. 567–574.
- [44] S. Brooks, A. Gelman, G. L. Jones, and X.-L. Meng, Eds., *Handbook of Markov Chain Monte Carlo*. Chapman & Hall/CRC, 2011.
- [45] M. Emzir, S. Lasanen, Z. Purisha, L. Roininen, and S. Särkkä, "Non-stationary multi-layered Gaussian priors for Bayesian inversion," *Inverse Problems*, vol. 37, no. 1, p. 015002, 2020.
- [46] I. Karatzas and S. E. Shreve, *Brownian Motion and Stochastic Calculus*, 2nd ed. Springer-Verlag New York, 1991, vol. 113.
- [47] S. Särkkä and A. Solin, *Applied Stochastic Differential Equations*. Cambridge University Press, 2019, vol. 10.
- [48] A. Solin and S. Särkkä, "Explicit link between periodic covariance functions and state space models," in *Proceedings of the 17th International Conference on Artificial Intelligence and Statistics*. Reykjavík, Iceland: PMLR, 2014, pp. 904–912.



- [49] P. E. Kloeden and E. Platen, *Numerical Solution of Stochastic Differential Equations*. Springer-Verlag Berlin Heidelberg, 1992.
- [50] Z. Zhao, T. Karvonen, R. Hostettler, and S. Särkkä, “Taylor moment expansion for continuous-discrete Gaussian filtering,” *IEEE Transactions on Automatic Control*, vol. 66, no. 9, pp. 4460–4467, 2021.
- [51] A. H. Jazwinski, *Stochastic Processes and Filtering Theory*. Academic Press, 1970.
- [52] K. Itô and K. Xiong, “Gaussian filters for nonlinear filtering problems,” *IEEE Transactions on Automatic Control*, vol. 45, no. 5, pp. 910–927, 2000.
- [53] S. Särkkä and J. Sarmavuori, “Gaussian filtering and smoothing for continuous-discrete dynamic systems,” *Signal Processing*, vol. 93, no. 2, pp. 500–510, 2013.
- [54] N. Chopin and O. Papaspiliopoulos, *An Introduction to Sequential Monte Carlo*. Springer International Publishing, 2020.
- [55] S. Särkkä, *Bayesian Filtering and Smoothing*. Cambridge University Press, 2013, vol. 3.
- [56] B. D. O. Anderson and J. B. Moore, “Detectability and stabilizability of time-varying discrete-time linear systems,” *SIAM Journal on Control and Optimization*, vol. 19, no. 1, pp. 20–32, 1981.
- [57] K. Reif, S. Günther, E. Yaz, and R. Unbehauen, “Stochastic stability of the discrete-time extended Kalman filter,” *IEEE Transactions on Automatic Control*, vol. 44, no. 4, pp. 714–728, 1999.
- [58] K. Xiong, H. Y. Zhang, and C. W. Chan, “Performance evaluation of UKF-based nonlinear filtering,” *Automatica*, vol. 42, no. 2, pp. 261–270, 2006.
- [59] T. Karvonen, S. Bonnabel, E. Moulines, and S. Särkkä, “On stability of a class of filters for nonlinear stochastic systems,” *SIAM Journal on Control and Optimization*, vol. 58, no. 4, pp. 2023–2049, 2020.
- [60] T. Ozaki, “A local linearization approach to nonlinear filtering,” *International Journal of Control*, vol. 57, no. 1, pp. 75–96, 1993.
- [61] J. Nocedal and S. J. Wright, *Numerical Optimization*, 2nd ed. Springer-Verlag New York, 2006.
- [62] B. P. Abbott *et al.*, “Observation of gravitational waves from a binary black hole merger,” *Physical Review Letters*, vol. 116, no. 6, p. 061102, 2016.
- [63] R. M. Liang and K. S. Arun, “Parameter estimation for superimposed chirp signals,” in *Proceedings of the 1992 IEEE International Conference on Acoustics, Speech, and Signal Processing*, vol. 5, 1992, pp. 273–276.
- [64] Z. Zhao, S. Särkkä, and A. B. Rad, “Kalman-based spectrotemporal ECG analysis using deep convolutional networks for atrial fibrillation detection,” *Journal of Signal Processing Systems*, vol. 92, no. 7, pp. 621–623, 2020.
- [65] S. Saha and S. M. Kay, “Sparse semi-parametric estimation of harmonic chirp signals,” *IEEE Transactions on Signal Processing*, vol. 50, no. 2, pp. 224–230, 2002.
- [66] Y. Bar-Shalom, X.-R. Li, and T. Kirubarajan, *Estimation with Applications to Tracking and Navigation*. Wiley, 2001.
- [67] R. Piché, S. Särkkä, and J. Hartikainen, “Recursive outlier-robust filtering and smoothing for nonlinear systems using the multivariate Student-t distribution,” in *Proceedings of the 2012 IEEE International Workshop on Machine Learning for Signal Processing*, 2012, pp. 1–6.
- [68] M. Roth, E. Özkan, and F. Gustafsson, “A Student’s t filter for heavy tailed process and measurement noise,” in *Proceedings of the 2013 IEEE International Conference on Acoustics, Speech and Signal Processing*, 2013, pp. 5770–5774.
- [69] F. Tronarp, R. Hostettler, and S. Särkkä, “Sigma-point filtering for nonlinear systems with non-additive heavy-tailed noise,” in *Proceedings of the 19th International Conference on Information Fusion*, 2016, pp. 1859–1866.
- [70] Y. Huang, Y. Zhang, N. Li, and J. Chambers, “Robust Student’s t based nonlinear filter and smoother,” *IEEE Transactions on*

*Aerospace and Electronic Systems*, vol. 52, no. 5, pp. 2586–2596, 2016.



**Zheng Zhao** received his D.Sc. degree from Aalto University, Espoo, Finland in 2021. He is currently working as a WASP postdoctoral researcher in the Department of Information Technology, Uppsala University, Sweden. His research interests include stochastic filtering, stochastic differential equations, Gaussian processes, signal processing, and machine learning.



verse problems.

**Simo Särkkä** received the M.Sc. (Tech.) and D.Sc. (Tech.) degrees from the Helsinki University of Technology, Espoo, Finland, in 2000 and 2006, respectively. He is currently an Associate Professor with Aalto University, Espoo, and an Adjunct Professor with the Tampere University and the LUT University. He is also affiliated with the Finnish Center of Artificial Intelligence (FCAI). His research interests include machine learning and multisensor data processing systems with applications in health and medical technology, location sensing, and in-



record as a prolific inventor with more than 25 patent applications.

**Jens Sjölund** received the B.Sc. and M.Sc. degree in engineering physics from the Royal Institute of Technology (KTH), Stockholm, Sweden, in 2010 and 2012, respectively, and the Ph.D. degree in biomedical engineering from Linköping University, Linköping, Sweden, in 2018. He is currently a WASP assistant professor of artificial intelligence with the Department of Information Technology, Uppsala University, Uppsala, Sweden. Prior to joining Uppsala University in 2021, he was a senior research scientist at Elekta, where he established a track



Royal Society of Sciences, Uppsala, Sweden. He was the recipient of the Tage Erlander Prize for natural sciences and technology in 2017 and the Arnerberg Prize in 2016, both awarded by the Royal Swedish Academy of Sciences (KVA).

**Thomas Schön** received the B.Sc. degree in business administration and economics, the M.Sc. degree in applied physics and electrical engineering, and the Ph.D. degree in automatic control from Linköping University, Linköping, Sweden, in January 2001, September 2001, and February 2006, respectively. He is currently the Beijer Professor of artificial intelligence with the Department of Information Technology, Uppsala University, Uppsala, Sweden. In 2018, he was elected to The Royal Swedish Academy of Engineering Sciences (IVA) and The